Moderation of near-field pressure over a supersonic flight model using laser-pulse energy deposition

D. Furukawa, Y. Aoki, A. Iwakawa, and A. Sasoh

Citation: Physics of Fluids **28**, 051701 (2016); doi: 10.1063/1.4950783
View online: http://dx.doi.org/10.1063/1.4950783
View Table of Contents: http://scitation.aip.org/content/aip/journal/pof2/28/5?ver=pdfcov
Published by the AIP Publishing

PHYSICS OF FLUIDS **28**, 051701 (2016)

Moderation of near-field pressure over a supersonic flight model using laser-pulse energy deposition

D. Furukawa, Y. Aoki, A. Iwakawa, and A. Sasoh[a)]
Department of Aerospace Engineering, Nagoya University, Furo-cho, Nagoya 464-8603, Japan

(Received 5 February 2016; accepted 3 May 2016; published online 17 May 2016)

The impact of a thermal bubble produced by energy deposition on the near-field pressure over a Mach 1.7 free-flight model was experimentally investigated using an aeroballistic range. A laser pulse from a transversely excited atmospheric (TEA) CO_2 laser was sent into a test chamber with 68 kPa ambient pressure, focused 10 mm below the flight path of a conically nosed cylinder with a diameter of 10 mm. The pressure history, which was measured 150 mm below the flight path along the acoustic ray past the bubble, exhibited precursory pressure rise and round-off peak pressure, thereby demonstrating the proof-of-concept of sonic boom alleviation using energy deposition. *Published by AIP Publishing.* [http://dx.doi.org/10.1063/1.4950783]

Sonic boom, as a representative physical phenomenon induced by supersonic flight, still remains a challenging problem both as fundamental fluid dynamics and for practical application. The pressure field induced by a supersonic flight body influences pressure signature even over far field of hundreds of times the body length. Because flow kinetic energy in a supersonic regime is high, even a small impact can result in large variation of flow properties; small change in the body shape can greatly affect the near-field pressure signature.[1,2] The influence of the impact on the near field remains for a long propagation distance because the self-modification function due to wave nonlinearity becomes weaker with decreasing wave strength in far field. For this reason, moderation of near-field flow can impact even on the far-field pressure signature. Because a supersonic flight influences over a wide range, which is referred to as a "sonic boom carpet," it is not efficient to try to modify the pressure signature on the ground; rather a strategy to modify the near field should be pursued so that the far-field pressure signature becomes acceptable.

"Energy deposition"[3] is a modern approach for modifying the aerodynamic performance of a supersonic body. Using lasers, microwaves, or electrical discharge, a certain amount of energy is deposited around a supersonic body in order to improve its aerodynamic performance. Adelgren *et al.*[4] experimentally visualized the interaction between a laser-pulse-induced thermal bubble and a standing shock wave. The pressure modulation is caused by the so-called "lens" effect in which the standing bow shock wave is extruded because of the expansion wave. Tretyakov *et al.*[5] demonstrated a supersonic drag reduction of 45% using repetitive laser pulses. Kim *et al.*[6] followed the same scheme with the improved efficiency of energy deposition as large as 10. Osuka *et al.*[7] and Tamba *et al.*[8] demonstrated that with repetitive laser-pulse energy deposition of up to 60 kHz, boundary layer separation and/or the so-called low-frequency shock oscillation could be suppressed. Zaidi *et al.* investigated the effect of energy deposition on sonic boom alleviation both experimentally and numerically;[9,10] their experiment was conducted using a supersonic wind tunnel. A laser-pulse-induced thermal spot was generated off-axis, upstream from the supersonic flight body by about one body length. The oblique shock wave is weakened as a result of interaction with the laser thermal spot. However, the observation window for the effect of the laser thermal spot was limited to the vicinity of the body; the pressure profile was predicted only by computational fluid dynamics, which yielded limited conclusions.

a)Electronic mail: sasoh@nuae.nagoya-u.ac.jp.

In this study, near-field pressure moderation was experimentally demonstrated using a laser-pulse-induced thermal bubble over a supersonic free-flight model, thereby obtaining clear impact on sonic boom alleviation.

The experiment was conducted in a rectangular-bore ballistic range with a size of 44 mm × 20 mm.[11,12] An aluminum alloy (A7075-T651) cylindrical model, which was 10-mm in diameter and 80.4-mm long with a conical nose of a full apex angle of 20° (mass of 9.9 g), was launched with a rectangular sabot made of polycarbonate (mass of 15.0 g). Using the in-tube catapult launch scheme,[12] the free-flight model was separated from the sabot in the sabot separation section before the muzzle and launched at a Mach number of 1.69 ± 0.02. Figure 1 shows the schematic illustration of the test section in the test chamber. The inside of the chamber was evacuated using a rotary pump down to the test air pressure of 68 kPa. A laser pulse from a transversely excited atmospheric (TEA) CO_2 laser (ML205, SLCR-Lasertechnik GmbH) was sent into the test chamber through a ZnSe window placed in an upper flange. The laser pulse was then focused with a 70-mm-diameter ZnSe lens with a focal length of 150 mm. The laser pulse energy effectively delivered to the focal point was 4.7 J. In the time variation of the laser pulse power, an initial 100-ns peak is followed by a modest second peak with a duration of about 3 μs. The irradiation of the laser pulse was triggered with an appropriate delay from a photodiode signal of the free-flight model passage. In the present experiment, the trigger signal was set so that the breakdown due to the laser pulse irradiation was initiated 111 mm before the free-flight model along its flight path.

At the test section in the 1.0-m-diameter stainless-steel test chamber, piezoelectric pressure transducers (113B28, rise time of 1 μs, PCB Inc.) are flush-mounted on a steel plate placed horizontally below the nominal flight path by 150 mm. In this paper, an increment in pressure from the value before the arrival of a shock wave is designated by Δp. The location of the pressure transducers was set so that one transducer, named "PT1," measured the history of Δp at the location where the acoustic ray from the nose passed the thermal bubble, whereas the other transducer, "PT2," measured one not affected by the thermal bubble. Here, the acoustic ray is approximately determined as a straight line that is normal to the Mach wave with a Mach number of 1.7 and originates in the tip of a flight model. The sequence of the formation of the thermal bubble after the laser-pulse-induced breakdown and the interaction between the standing shock wave around the free-flight model and the thermal bubble were visualized with a shadowgraph system including a high-speed framing camera (HPV1, Shimadzu Co.) and a flash lamp (200J/Flash, 3 ms, SA-200F, Nissin Electronics Co., Ltd.).

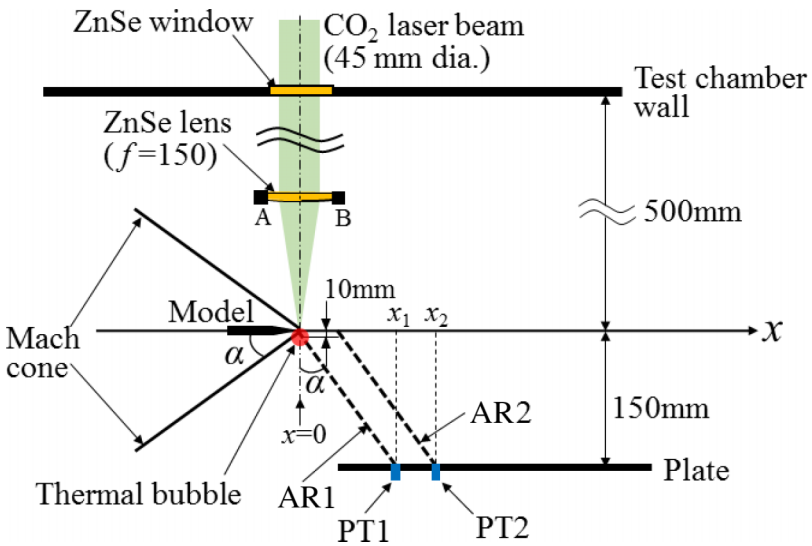

FIG. 1. Side view of test section, AR, acoustic ray; focal point of laser beam at 10 mm below the flight path on which x-axis is set.

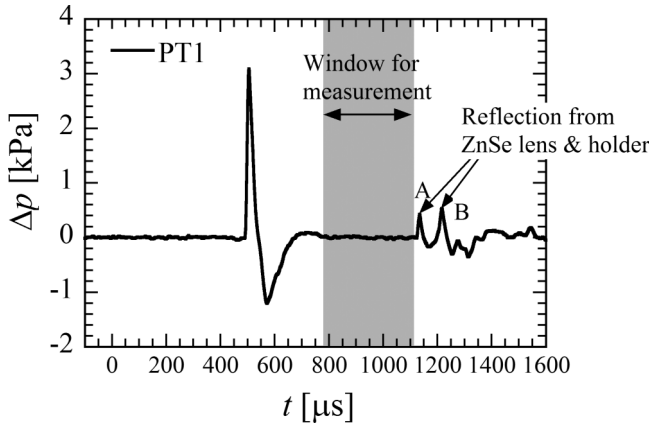

FIG. 2. Δp history measured at PT1 without free flight and only with energy deposition. The incident laser pulse energy was 4.53 J, and the ambient pressure was 68 kPa.

Figure 2 shows a Δp history measured by PT1, which is induced only by the laser-pulse irradiation without model flight. The time, t, originated at the moment the trigger signal is sent to the laser-pulse irradiation. The internal delay for the laser oscillator and the time duration required for the laser beam to travel from the laser head to the focal point in the test section were 1.9 μs and 27 ns, respectively. The first positive-to-negative pulses during 490 μs $< t <$ 800 μs were caused by a laser-pulse-driven blast wave. After the effective passage of the blast wave, Δp was restored to almost the initial value for 800 μs $< t <$ 1100 μs. This period is the time window available for measuring the near-field pressure history induced by a supersonic free-flight model, which is therefore indicated in the figure as the "window for measurement." At t = 1130 μs and 1200 μs, Δp peaks appear. These peaks are caused by the reflection of the laser-induced blast wave against the ZnSe lens. The first peak corresponds to the outer surface of the right side of the lens holder (Point B in Fig. 1), and the second peak corresponds to the inner surface of the left side of the lens holder (Point A in Fig. 1), as shown in Fig. 2. After this period, the Δp fluctuated due to pressure waves reflecting from various surfaces including the test chamber inner wall. Therefore, in the present experiment, the laser pulse irradiation was time controlled so that the shock/pressure waves induced by the free-flight model arrived at the pressure transducers during the respective window for measurement.

Figure 3 (Multimedia view) shows shadowgraph images of the interaction between the shock wave and the associated flow induced by the free-flight model and the laser-induced thermal bubble. The flight path is horizontal, from left to right. At t = 100 μs (Fig. 3(a) (Multimedia view)), the laser-pulse-induced blast wave barely touches the apex of the free-flight model. A thermal bubble has been already formed at the location of the breakdown. During the flow visualization period shown in Fig. 3 (Multimedia view), the roughly estimated diameter of the thermal bubble remained almost constant at about 27 mm. As is often observed in the evolution of a laser-pulse-induced thermal bubble, its shape is not perfectly spherical. However, for the purpose of the present investigation, this asymmetry does not violate the generality of the results. At t = 156 μs (Fig. 3(b) (Multimedia view)), the model becomes closer to the bubble but has not yet touched it. The model has already penetrated through the bubble at t = 212 μs (Fig. 3(c) (Multimedia view)). In the thermal bubble, the shock wave is not visible because of weak image contrast. However, due to interaction with the bubble, the standing conical shock wave should advance ahead of the wave from the apex. At t = 268 μs (Fig. 3(d) (Multimedia view)), the model was in the middle of the thermal bubble. Part of the Mach-cone-line of the leading shock wave is still in the image.

Figure 4 compares Δp histories with and without energy deposition measured by the pressure transducers shown in Fig. 1, PT1 in Fig. 4(a), and PT2 in Fig. 4(b). The acoustic ray incident on PT1 passed the thermal bubble, while that incident on PT2 did not. The abscissa, Δt, is defined so that the origin of each Δp history begins at the moment at which a leading shock wave or

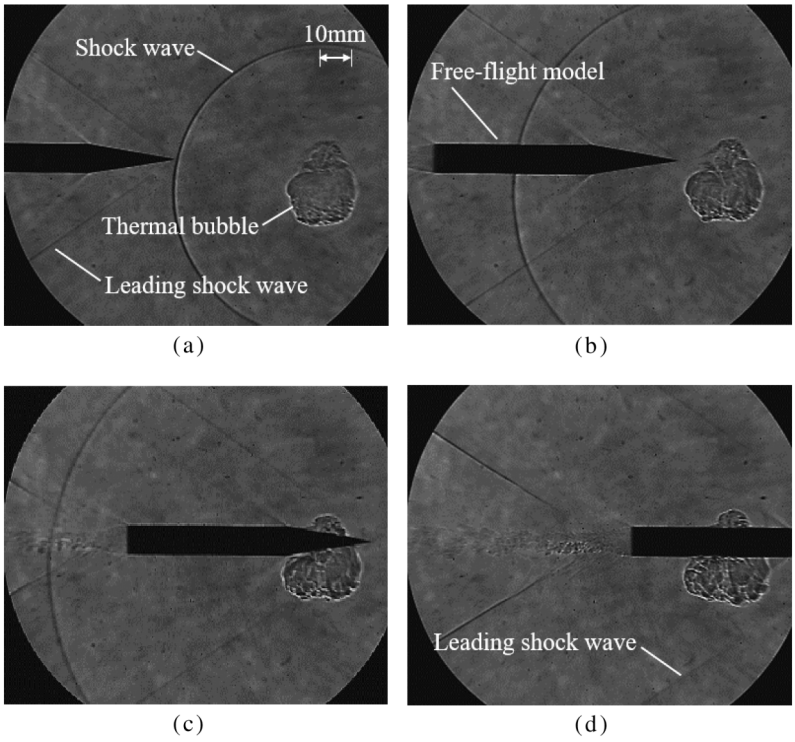

FIG. 3. Framing shadowgraph images around a supersonic free-flight model with a thermal bubble. (a) $t = 100$ [μs], (b) $t = 156$ [μs], (c) $t = 212$ [μs], (d) $t = 268$ [μs]. (Multimedia view) [URL: http://dx.doi.org/10.1063/1.4950783.1]

its equivalent arrived at a pressure transducer. Without energy deposition and/or in the case of PT2, Δp did not vary before the arrival of the oblique shock wave that originated at the apex of the free-flight model at $\Delta t = 0$ ms. Because the pressure transducers were mounted side-on with respect to the free-flight path, the effective rise time corresponding to the passage of the oblique shock wave equals the effective diameter of the transducer head divided by the flight speed, that is, 5.54×10^{-3} m/(1.7 × 340 m/s) = 9.6 μs. The experimental values of the effective rise time at

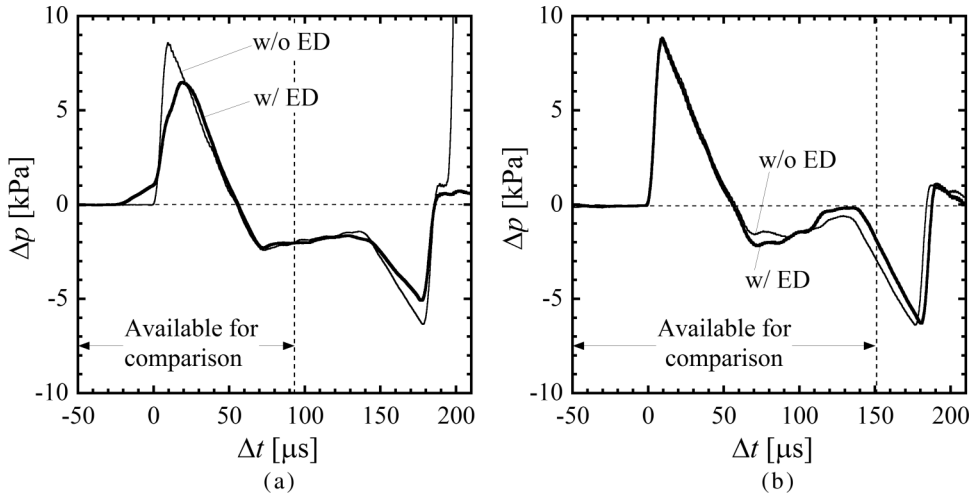

FIG. 4. Δp histories PT1 with the acoustic ray past the thermal bubble and PT2 off the thermal bubble. Vertical lines indicate the moment that expansion waves from the leading edge of the horizontal steel plate started affecting the Δp history, ED; laser energy deposition. (a) PT1, (b) PT2.

$\Delta t = 0$ ms are of the same order in magnitude. In this experiment, the distance from the leading edge of the steel plate to PT1 and PT2 is 80 mm and 130 mm, respectively; Δp signals that are measured by their respective transducers are contaminated by expansion waves from the leading edge for $\Delta t > 93$ μs and $\Delta t > 151$ μs. The boundaries of the respective time windows are indicated by vertical broken lines in Fig. 4.

In Fig. 4(a), Δp history at PT1 was greatly affected by the thermal bubble. Without energy deposition, the pressure increment past the oblique shock wave measured equaled 8.0 kPa. After the oblique shock wave, Δp decreased almost linearly with time, even down to negative values. At $\Delta t = 180$ μs, Δp started increasing again, thereby forming an "N" shape. With the laser energy deposition, the Δp history started slowly rising to 1.0 kPa before the primary oblique shock wave arrived, -29 μs $< \Delta t < 2$ μs. The pressure rise of the primary shock wave was dispersed into two separate increases, first from 1.0 to 3.6 kPa starting at $\Delta t = 8$ μs and second from 3.6 to 6.0 kPa at 23 μs. During 25 μs $< \Delta t < 75$ μs, the two Δp signals monotonically decreased, approaching each other. During this period, the effect of the thermal bubble in the post-shock flow gradually weakened. For 90 μs $< \Delta t$, comparing the two histories does not make meaningful sense because Δp signal of PT1 is contaminated by expansion waves from the leading edge of the steel plate.

The location of PT2 is far from the ray passing through the thermal bubble. The Δp histories well reproduced that of PT1 without laser energy deposition; the first pressure rises of the primary interest agree well with each other, although due to wake behavior small differences appeared for $t > 65$ μs.

Here, the wave dispersion effect due to the thermal bubble is estimated from the time difference in the wave arrival time through the thermal bubble and off the thermal bubble. As shown in Fig. 3(a), the characteristic diameter of the thermal bubble, d_f, equals 27 mm. We assume that a spherical region of air with a diameter of d_i absorbed the laser pulse energy E with a constant volume and an effective absorption coefficient η. Then, the heated sphere increased its diameter to d_f in an isentropic manner with a constant specific heat ratio of $\gamma = 1.4$. In this rule of thumb estimation, we assume from previous experience that $\eta = 0.3$.[13] Substituting experimental values, $E = 4.7$ J and $d_f = 27$ mm, and d_i is 19 mm. This value is the same order as the characteristic diameter of the laser-heated region observed using high-speed shadowgraph photography (not shown here) with an increased time resolution of 100 ns. If we employ these values, the characteristic temperature in the thermal value equals 890 K compared with the initial temperature of 290 K. Therefore, the characteristic arrival time for the precursory wave advancing against the same path without the thermal bubble equals 34 μs. This value is in the same order as of the value measured in Fig. 4(a).

In this study, Δp induced by the standing shock wave formed around the supersonic free-flight model was moderated using a laser-pulse-induced thermal bubble formed in the flight path. The Δp history experienced a precursory period ahead of the nominal shock wave arrival and dispersion into two Δp peaks with weakened levels. The characteristic period of shock wave dispersion in the precursory shock wave agrees with the assumption that the standing shock wave experiences dispersion through the bubble due to its higher speed of sound. This demonstration suggests the possibility of active "spot" sonic boom alleviation during a supersonic flight over a specific target in order to avoid acoustic hazards.

The authors appreciate valuable suggestions from Dr. Bing Wang on the generation of the laser-pulse induced thermal bubble. Technical assistance was provided by Mr. D. Yoshimizu, undergraduate student, Mr. A. Saito, Mr. K. Yamamoto, and Mr. N. Shiraki, Technical Division, Nagoya University. This study was supported by the Japan Society for Promotion of Science as a Grant-in-Aid for Scientific Research (A) No. 15H02321.

[1] R. Seebass and A. R. George, "Sonic boom minimization," J. Acoust. Soc. Am. **51**, 686–694 (1972).
[2] D. C. Howe, F. Simmons III, and D. Freund, "Development of the gulfstream quiet spike for sonic boom minimization," AIAA Paper 2008-0124, 2008.
[3] D. Knight, "Survey of aerodynamic drag reduction at high speed by energy deposition," J. Propul. Power **24**, 1153–1167 (2008).
[4] R. A. Adelgren, H. Yan, G. S. Elliott, D. D. Knight, T. J. Beutner, and A. A. Zheltovodov, "Control of Edney IV interaction by pulsed laser energy deposition," AIAA J. **43**, 256–269 (2005).

[5] P. K. Tret'yakov, A. F. Garanin, G. N. Grachev, V. L. Krainev, A. G. Ponomarenko, V. N. Tishchenko, and V. I. Yakovlev, "Control of supersonic flow around bodies by means of high-power recurrent optical breakdown," Phys.–Dokl. **41**, 566–567 (1996).
[6] J.-H. Kim, A. Matsuda, T. Sakai, and A. Sasoh, "Wave drag reduction with acting spike induced by laser-pulse energy depositions," AIAA J. **49**, 2076–2078 (2011).
[7] T. Osuka, E. Erdem, N. Hasegawa, R. Majima, T. Tamba, S. Yokota, A. Sasoh, and K. Kontis, "Laser energy deposition effectiveness on shock-wave boundary-layer interactions over cylinder-flare combinations," Phys. Fluids **26**, 096103 (2014).
[8] T. Tamba, H. S. Pham, T. Shoda, A. Iwakawa, and A. Sasoh, "Frequency modulation in shock wave-boundary layer interaction by repetitive-pulse laser energy deposition," Phys. Fluids **27**, 091704 (2015).
[9] S. H. Zaidi, M. N. Shneider, and R. B. Miles, "Shock-wave mitigation through off-body pulsed energy deposition," AIAA J. **42**, 326–331 (2004).
[10] M. N. Shneider, S. O. Macheret, S. H. Zaidi, I. G. Girgis, and R. B. Miles, "Virtual shapes in supersonic flow control with energy addition," J. Propul. Power **24**, 900–915 (2008).
[11] A. Sasoh, K. Kikuchi, K. Shimizu, and A. Matsuda, "Aluminum-extrusion, square-bore, aero-ballistic range for launching three-dimensional projectiles," Int. J. Aerosp. Innovations **2**, 147–156 (2010).
[12] A. Sasoh, T. Imaizumi, A. Toyoda, and T. Ooyama, "In-tube catapult launch from rectangular-bore aeroballistic range," AIAA J. **53**, 2781–2784 (2015).
[13] J.-Y. Choi, A. Sasoh, I.-S. Jeung, N. Urabe, and H. Kleine, "Impulse generation mechanisms in laser-driven in-tube accelerator," Trans. Jpn. Soc. Aeronaut. Space Sci. **51**(172), 71–77 (2008).